Materials Research, Vol. 3, No. 2, 31-35, 2000.

Influence of the Microstructure of Duplex Stainless Steels on their Failure Characteristics During Hot Deformation

G.S. Reis, A.M. Jorge Jr., O. Balancin*

Departamento de Engenharia de Materiais, Universidade Federal de São Carlos, 13565-905 São Carlos - SP, Brazil

Received: July 20, 1999 Revised: February 11, 2000

Two types of duplex stainless steels were deformed by torsion at a temperature range of 900 to 1200 °C and strain rate of 1.0 s^{-1} and their final microstructures were observed. The austenite volume fraction of steel A (26.5Cr - 4.9Ni - 1.6Mo) is approximately 25% at room temperature, after conventional annealing, while that of steel B (24Cr - 7.5Ni - 2.3Mo) is around 55%. Experimental data show that steel A is ductile at high temperatures and displays low ductility at low temperatures, while steel B has low ductility in the entire range of temperatures studied. At high temperatures, steel A is essentially ferritic and shows dynamic recrystallized grains after deformation. When steel A is strained at low temperatures and displays low austenite volume fraction, microstructural observations indicate that failure is triggered by grain boundary sliding due to the formation of an austenite net structure at the ferrite grain boundaries. At intermediate volume fraction, when austenite forms a dispersed second-phase in steels A and B, failure begins at the ferrite/ferrite boundaries since some of the new ferrite grains may become immobilized by the austenite particles. When steel B is strained at volume fraction of around 50% of austenite and both phases percolate the microstructure, failure occurs after low straining as a consequence of the different plastic behaviors of each of the phases. The failure characteristics of both steels are correlated not only with the volume fraction of austenite but also with its distribution within the ferrite matrix, which limits attainable strain without failure.

Keywords: *duplex stainless steel, hot working, hot ductility*

1. Introduction

Duplex stainless steels have become more attractive than single-phase austenitic and ferritic grades in many industrial applications owing to their high strength and corrosion resistance in chloride-containing media[1,2]. Although advantageous, the processing of these materials requires special attention due to the existence of a low ductility region under hot working conditions[3]. Generally, the presence of a massive second phase during processing makes deformation more complex and the microstructure is a decisive limiting factor on plastic behavior. In addition to the work hardening and softening mechanisms required to deform each phase, the boundaries play an important role in duplex microstructures; the accommodation of macroscopic deformation depends on the plastic characteristics of both phases and interfaces[4,5].

It is a well known fact that during high temperature deformation, after a certain amount of work hardening, single phase ferritic stainless steels soften by intense dynamic recovery while austenitic stainless steels, with relatively low stacking fault energy, soften by dynamic recrystallization[6,7]. When the two phases are jointly deformed, the distribution of strains among the phases is no longer uniform. When straining begins in duplex stainless steels, strain concentrations appear in the softer ferrite phase. As deformation increases, strain gradients may decrease as a result of accommodation mechanisms such as recovery and recrystallization, cracking formation, as well as interphase and grain boundary sliding.

In spite of the complex deformation behavior of duplex stainless steels, it has been found that the ferrite phase continues to show intense dynamic recovery while the austenite phase undergoes dynamic recrystallization[8-10]. Thus, ferrite and austenite display dissimilar behaviors and microstructures during high temperature deformation, limiting attainable strain without failure. Recent research has shown that the ductility of this kind of steel depends on the

* balancin@power.ufscar.br

deformation conditions, the behavior of the constituent phases, and the volume fraction of austenite in the ferrite matrix[9,11,12]. Also, it has been suggested that the ductility of duplex steels depends on phase distribution and on the nature of the interface between these phases[5,9]. Although attention has been paid to the softening mechanisms of the ferrite and austenite phases and on deformation conditions, very few systematic studies have focussed on the identification of the relationship between the microstructure and failure characteristics of these steels during high temperature deformation.

The purpose of this work was to observe the failure characteristics during hot deformation of two-phase alloys relating then to the different microstructures which were present. In order to obtain a large number of initial microstructures, two kinds of duplex stainless steels were strained by torsion tests under various deformation conditions after two initial thermal treatments.

2. Materials and Experimental Procedures

Two types of two-phase alloys with different Cr/Ni equivalent ratios were investigated in this work. The austenite volume fraction of steel A (26.5Cr - 4.9Ni - 1.6Mo) is around 25% at room temperature, after conventional annealing and cooling, while that of steel B (24Cr - 7.5Ni - 2.3Mo) is approximately 55%. Figure 1 illustrates the cross section of the Fe-Cr-Ni system with 70% Fe and indicates the constituent phases expected for these steels after equilibrium is achieved during reheating at high temperatures before deformation. Although the ferrite/austenite ratio changes with temperature, steel B always contains more austenite than steel A under similar reheating and deformation conditions.

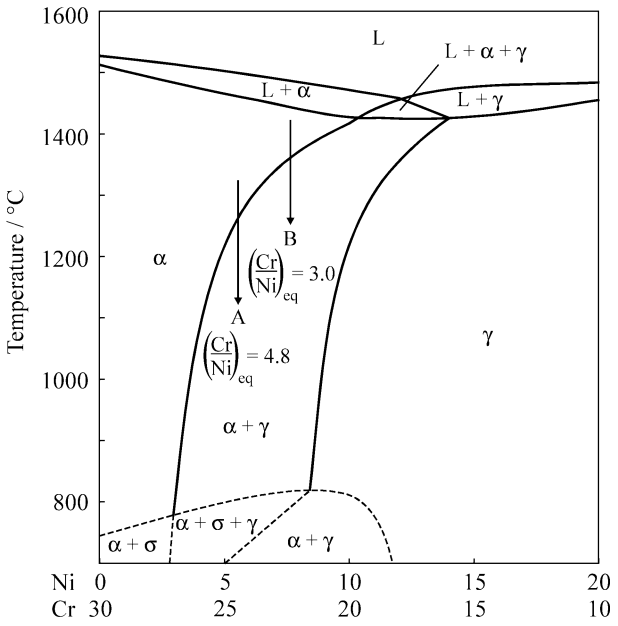

Figure 1. Cross section of the Fe-Cr-Ni system with 70% Fe[13]. The relative locations of steels A and B were determined taking into account the Cr/Ni equivalent ratios.

Mechanical tests were carried out on a computerized hot torsion machine described previously[14]. The samples were 10-mm in length and 10-mm in diameter in the reduced central gage section. These were heated by means of an induction furnace assembled on the testing machine. Chromel-alumel thermocouples were used to control the power supply to the furnace and to monitor the specimen temperature during testing. To retain the high temperature microstructures for further observations, water was injected into a quartz tube surrounding the sample, immediately upon reaching the fracture strain. After standard metallographic procedures, a deposition color etch composed of 100 mL distilled H_2O, 20 mL HCl and 2 g potassium metabissulfite was applied, in order to observe the microstructure.

Hot torsion tests were carried out over a 900 to 1200 °C temperature range, at an equivalent strain rate of 1 s^{-1}. Some of the tests were conducted after heating to 1250 °C and then cooling to deformation temperature, and others after heating to test temperature only, in order to produce a variety of microstructures before deformation.

The temperatures required for complete dissolution of the austenite were estimated at around 1250 °C for steel A and above 1300 °C for steel B (see Fig. 1). It was, therefore, expected that all the austenite was dissolved during the treatment at 1250 °C in steel A and somewhat less in steel B. In tests carried out on heating, the austenite volume fraction decreased as the temperature rose, until the material was almost entirely ferritic at solution temperature. As the temperature was reduced to below the reheat temperature on cooling, the phase transformation began with the nucleation and growth of the austenite phase in the grains and at the ferrite grain boundaries.

3. Results

Ductility was evaluated measuring the strain to fracture from flow curves obtained from torsion tests. Figure 2 shows the dependence of the strain to fracture on deformation temperature for steel A, samples tested on cooling and on heating, and for steel B, samples tested on cooling only. Steel A is very ductile at high temperatures, but its ductility decreases with decreasing test temperature. As the volume fraction of austenite in the ferrite matrix increases, ductility also decreases; that is the reason steel B exhibits such low ductility over the entire temperature range.

Figure 2 shows three different behaviors in the dependence of ductility on test temperatures: (i) steel A is very ductile at high temperatures; (ii) steel A has low ductility at low temperatures, regardless of the previous thermal treatment; and (iii) steel B has low ductility in the entire range of temperatures studied.

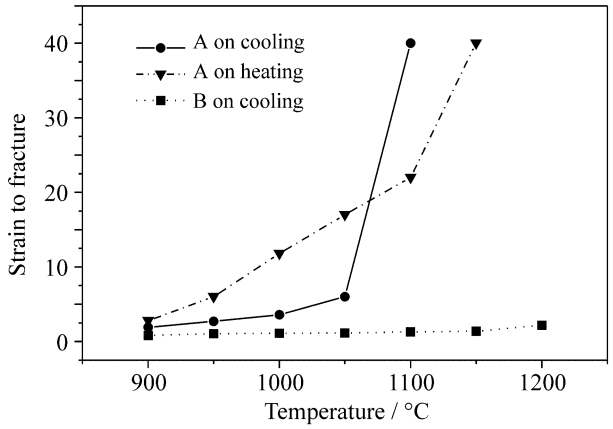

Figure 2. Dependence of strain to fracture on deformation temperature for steels A and B.

At high temperatures, as illustrated in the diagram of Fig. 1, steel A is essentially ferritic. An example of this kind of microstructure is given in Fig. 3. In this case, the sample was tested on cooling to 1100 °C and strained to $\varepsilon = 1.2$. The microstructure consisted of the small new grains in the old ferrite grains; initial grains of 400 μm were reduced to about 20 μm. This leads to the conclusion that dynamic recrystallization occurred, although this material tends to soften by intense dynamic recovery. Previous studies on ferrite stainless steel[15] and α - iron[16] show that continuous dynamic recrystallization takes place in these materials after large deformation, with the formation of new grains deriving from the growth of subgrains and a gradual increase in sub-boundary misorientation. Also, it is worth observing in Fig. 3 that the old grain boundaries were bulged by the grains formed during deformation.

Figure 4 shows the microstructure of a steel A sample tested on cooling to 950 °C and strained until it fractured ($\varepsilon = 2.5$). The microstructure consists of a ferrite matrix containing austenite particles within the grains and at grain boundaries. The volume fraction of austenite is small ($F_v \sim 5\%$) since the sample was heated to 1250 °C, which is higher than the austenite solution temperature, cooled to test temperature and strained before the equilibrium volume fraction of austenite was attained. In this case, deformation conditions represent the behavior (ii) described above. This figure clearly shows the formation of cracks at ferrite grain boundaries, indicating that the failure process is triggered by grain boundary sliding.

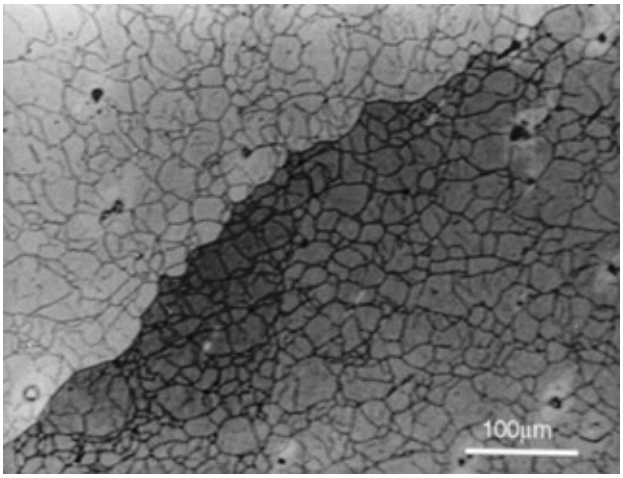

Figure 3. Microstructure of steel A tested on cooling to 1100 °C, displaying new ferrite grains formed by continuous dynamic recristallization after straining to $\varepsilon = 1.2$.

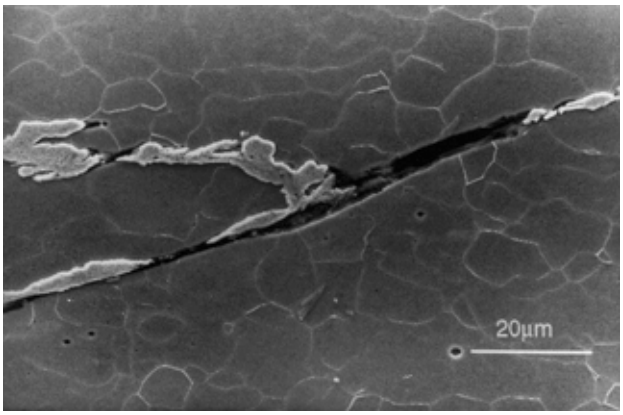

Figure 4. Steel A tested on cooling to 950 °C, displaying formation of cracks by grain boundary sliding after straining to $\varepsilon = 2.5$.

Figure 5 presents the microstructure of a sample with intermediate austenite volume fraction. This was obtained from steel A tested on heating to 950 °C and strained to $\varepsilon = 6.0$. The microstructure consists of a ferrite matrix containing a volume fraction of around 20% of austenite. Ferrite grains, formed as a result of dynamic recrystallization, are small and equiaxial, while austenite particles are elongated and aligned in the direction of deformation. This micrography also shows the formation of some cracks at interphase boundaries, although most of them are located at the ferrite/ferrite boundaries.

When the volume fraction of austenite is increased, the structure of the material tends to become duplex. Figure 6

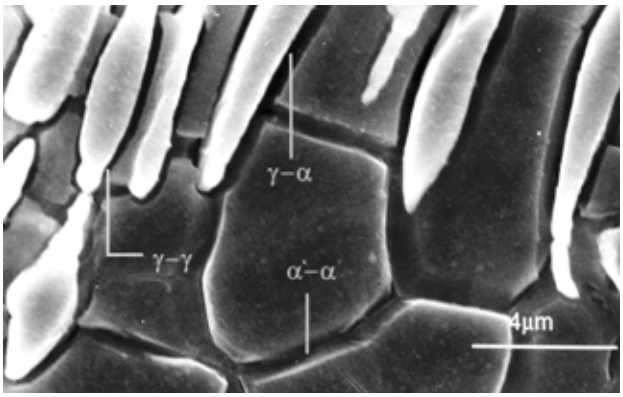

Figure 5. Microstructure of steel A strained at 950 °C on heating, showing cracking at ferrite/ferrite boundaries.

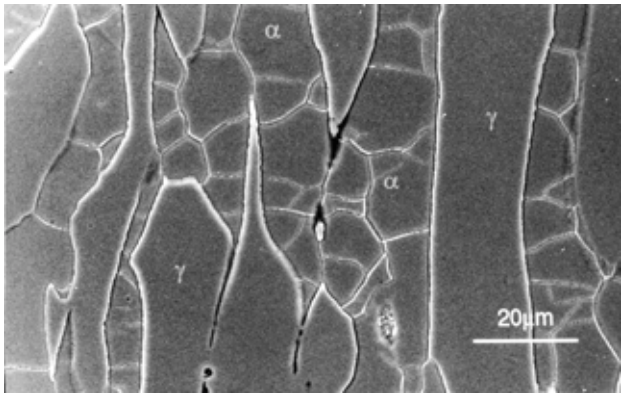

Figure 6. Microstructure of steel B tested on cooling to 1100 °C, showing the formation of cracks after straining to ε = 1.3.

shows the microstructure of a steel B sample obtained after straining to ε = 1.3 and tested on cooling to 1100 °C. The volume fraction of austenite is close to 50% and the microstructure consists of alternating austenite and ferrite phases aligned in the direction of deformation. The austenite reveals coarse elongated grains, typical of the work hardening regime, while the ferrite displays fine equiaxial grains that characterize its dynamic recrystallization. This figure also shows the formation of cracks at ferrite/austenite interfaces, and on ferrite/ferrite and austenite/austenite grains.

4. Discussion

Two steels were used in this investigation, two different initial thermal treatments were applied, and various deformation conditions were used. As a result of the variety of conditions employed, a large number of initial microstructures was obtained. These ranged from single phase ferrite to mixtures of ferrite and austenite with several volume fractions, distributions and austenite particle shapes.

When steel A is tested at high temperatures (above 1100 °C), it is essentially ferritic and highly ductile. It would appear that the high ductility obtained in these experiments may be attributed to two causes: i) one is the ease of dislocation annihilation and of sub-boundary formation, which decrease the material's strength; ii) the second cause is the bulging and motion of high angle grain boundaries, which have the beneficial effect of isolating the cracks formed at original boundaries and of inhibiting grain boundary sliding[17].

As the temperature is decreased and particles of austenite are observed in the matrix, so ductility decreases. Figure 2 shows that, at 950 °C, steel A can be strained to 2.5 on cooling and 6.0 on heating without failure as compared to strains of about 40 at 1100 °C. From Figs. 4 and 5 it can be observed that the volume fraction of austenite is larger in the heat tested sample than in the cooling tested one. Hence, one can infer that the level of ductility is correlated not only to the volume fraction of austenite but also to its distribution within the ferrite matrix.

The sample tested on cooling was heated to above the austenite dissolution temperature and then cooled to test temperature. Although at 950 °C the equilibrium volume fraction of austenite is relatively high, the time spent on cooling was insufficient for the alfa-gamma transformation to be completed, allowing for the observation of only a small volume fraction of austenite. Figure 2 shows that most of the austenite phase is located at the ferrite grain boundaries, forming a thin film that characterizes a net structure[18]. The failure process occurs by grain boundary sliding, which is independent of the austenite volume fraction in the ferrite matrix.

When tests are carried out with the on heating samples, part of the austenite that is present at room temperature is dissolved before deformation. As diffusion is easier at the boundaries than inside the grains, the austenite dissolution begins on the film at the grain boundaries. After some time of reheating, the ferrite grain boundaries are no longer covered by a continuous film of austenite. This inhibits grain boundary sliding and continuous dynamic recrystallization proceeds to increase ductility. Thus, the ferrite matrix flows around the harder austenite phase, which acts as a dispersed second phase. After large deformations, austenite particles constrain the motion of the new grains and failure begins with cracking at the ferrite/ferrite boundaries (see Fig. 5).

As the volume fraction of austenite is increased further and the microstructure is characterized by ferrite and austenite percolation[18], the plastic behavior depends on both the phases. Because the diffusion rates in ferrite are about one order of magnitude higher than in austenite and the dislocation movement in ferrite is much faster due to its high stacking fault energy, ferrite and austenite display dissimilar behaviors during high temperature deformation. When straining starts, the softer ferrite phase deforms plastically to a larger extent than the harder austenite. After some work hardening, the ferrite softens while the austenite begins working hardening. Thus, the ferrite matrix flows alongside the harder austenite phase, forming cavities at triple junctions and at ferrite/austenite interfaces parallel to the direction of shear (see Fig. 6), which greatly decreases ductility.

To confirm that this sharp decrease in ductility is associated with the microstructure, a complementary experiment was carried out using steel B, in which the austenite particles are no longer contiguous (Fig. 7). This sample was tested on cooling to 1200 °C after reheating to 1350 °C for 30 min. The micrography displays cracking at ferrite/ferrite boundaries, indicating that the austenite particles constrain the motion of the recrystallized ferrite grains, which is typical of dispersed second-phase behavior. The strain to fracture was 4.8, *i.e.*, 3.4 times the value obtained at the same temperature when both phases percolate.

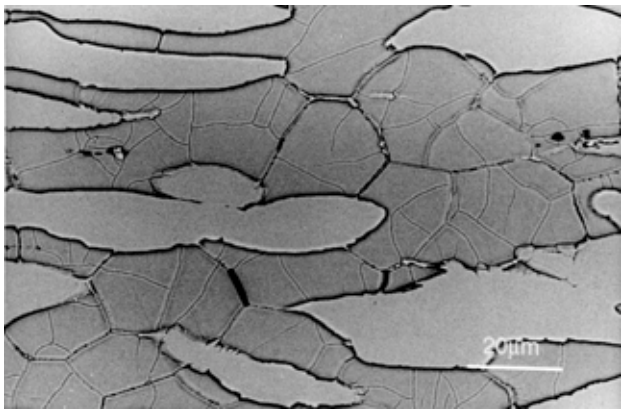

Figure 7. Microstructure of steel B tested on cooling to 1200 °C after reheating to 1350 °C.

5. Conclusions

- The ductility of duplex stainless steels depends on the deformation temperature and volume fraction of austenite, and it is also sensitive to austenite particle distribution.

- These materials are very ductile at high temperatures if very low austenite volume fraction is present.

- When the second phase forms a net structure, material failure occurs by grain boundary sliding after little straining, regardless of the volume fraction of austenite.

- When the austenite is distributed as a dispersed second phase, ductility increases and failure is caused by austenite particles that immobilize the new ferrite grains formed by dynamic recrystallization.

- As the volume fraction of austenite increases and the microstructure is characterized by percolation of both phases, failure occurs after low straining as a result of the different plastic behaviors of each phase, regardless of test temperatures.

Acknowledgements

The financial support of the Brazilian agencies FAPESP, CAPES and CNPq are gratefully acknowledged.

References

1. Solomon, H.D.; Devine Jr, T.M. Duplex Stainless Steels. ASM, Metals Park, Ohio (R.A. Lula, ed.), p. 693, 1982.
2. Nilsson, J.O. *Mater. Sci. Tech.*, v. 8, p. 685, 1992.
3. Kawasaki, T.; Takada, I.; Ohtsubo, H.; Suzuki, S. *Kawasaki Steel Technical Report* n. 14, p. 50, 1986.
4. Akdut, N.; Foct, J. ISIJ International, v. 36, p. 883, 1996.
5. Iza-Mendia, A.; Pinõl-Juez, A.; Urcola, J.J.; Gutiérrez, I. *Metall. Mat. Trans.*, v. 29A, p. 2975, 1998.
6. Richards, P.; Sheppard, T. *Mat. Sci. Tech.*, v. 2, p. 836, 1986.
7. McQueen, H.J.; Ryan, N.D.; Evangelista, E. *Mat. Sci. Forum*, v. 113-115, p. 435, 1993.
8. Wang, R.; Lei, T.C. *Mat. Sci. Eng.*, A165, p. 19, 1993.
9. Arboledas, J.B.; Tirado, J.L.M.; Rodriguez, R.S. *Proc. Int. Congress Stainless Steels'96*, p. 116. Dusseldorf/Neuss, June, 1996.
10. Cizek, P.; Wynne, B.P. *Mat. Sci. Eng.*, A230, p.88, 1997.
11. Hoffmann, W.A.M.; Balancin, O. *Informacion Tecnologica*, v. 9, p. 11, 1998.
12. Mecozzi, M.G.; Capotosti, L. *Proc. Int. Congress Stainless Steels'96*, p. 317. Dusseldorf/Neuss, June, 1996.
13. Pugh, J.W.; Niebest, J.O. *Trans. AIME*, v. 188, p. 268, 1950.
14. Jorge-Jr., A.M.; Balancin, O. *Revista de Engenharia e Ciências Aplicadas*, v. 2, p. 133, 1994/1995.
15. Belyakov, A.; Kaibyshev, R.; Zaripova, R. *Mat. Sci. Forum*, v. 113-115, p. 385, 1993.
16. Baczynski, J.; Jonas, J.J. *Metall. Mater. Trans.*, v. 29A, p. 447, 1998.
17. McQueen, H.J.; Ryan, N.D.; Konopleva, E.V.; Xia, X. *Can. Metall. Quart.*, v. 34, p. 219, 1995.
18. Hornbogen, E. *Acta Metall.*, v. 32, p. 615, 1984.